

Interaction of Piperidin Derivative of Mannich Base with DPPC Liposomes

Katarzyna Cieřlik-Boczula,^{*,†} Rafał Michał Petrus,[†] Gottfried Köhler,[‡] Tadeusz Lis,[†] and Aleksander Koll[†][†]Faculty of Chemistry, University of Wrocław, Joliot-Curie 14, 50-383 Wrocław, Poland[‡]Max F. Perutz Laboratories, Department of Computational and Structural Biology, University of Vienna, Campus Vienna Biocenter 5/1, Vienna 1030, Austria

S Supporting Information

ABSTRACT: The long chain Mannich bases, especially with the piperidine and morpholine groups, display very promising antimicrobial activity. In order to extend our knowledge on their impact on biological systems, we examined the interactions of the 5-pentadecyl-2-((piperidin-1-yl)methyl)phenol (PPDP) with model lipid membrane by means of differential scanning calorimetry (DSC) and fluorescence measurements. The small unilamellar vesicles of dipalmitoylphosphatidylcholine (DPPC) with different piperidine Mannich base concentration were investigated as a function of the increase of temperature. The phase separation accompanied by the rise of the transition enthalpy of both subcomponents, the increase of the function of the GP values of Laurdan versus the wavelength of excitation in the gel phase of PPDP/DPPC systems, and no remarkable differences in the fluorescence anisotropy of PPDP molecules in lipid environment for different mixtures of PPDP/DPPC was observed. Additionally, it was shown that PPDP itself interdigitated in solid state.



Piperidin derivative of Mannich base can modulate physicochemical properties of lipid membrane

1. INTRODUCTION

The Mannich bases, which have been reported as potential biological agents, find an extraordinarily wide pharmaceutical application as antitubercular,¹ antimalarial,² vasorelaxing,³ analgesic,⁴ and anticancer drugs.⁵ They exhibited activity against Maurine P388 lymphocytic leukemia (Wi Dr Colon cancer) *in vitro*.⁶ The long-chain derivatives play an important role in the emulsification process.⁷ Moreover, a new trend in the Mannich base actions appeared in their biocidal activity toward various types of microorganisms. It was shown that the long chain Mannich bases, especially with piperidine and morpholine as the secondary amine moiety, exhibit a very high biocidal activity toward Gram positive bacteria (*Staph. Cocu.*, *Bacillus*), Gram negative bacteria (*Salmonella*, *E. coli*), fungi (*A. terrus*, *A. flavus*), and yeast (*Candida*).⁸ In this paper, we have studied 5-pentadecyl-2-((piperidin-1-yl)methyl)phenol (PPDP), which is a new example of the long chain Mannich base.

The biocidal activity of the Mannich bases depends mainly on the chemical structure and their surface activity.⁹ The antipatogenic action can be explained on the basis of the superior ability of long tail Mannich bases to cross the lipid membrane, mainly because of their lipophilic nature and binding with the receptor sites. They anchor by its tail in the hydrophobic core of the lipid bilayer, whereas a more polar "head" is exposed to the surface of the membrane. The presence of the Mannich bases in the cell membrane may cause the effective resistance against the different types of microorganisms. The first step of many infections is the formation of a direct contact between a pathogen and the plasma membrane of host cells. Thus, the cells of bacteria and fungi could have

direct contact with the Mannich compounds if they were located in the membrane of the host cells. On the other hand, there is a question if these molecules have any effect on the membrane structure and other physicochemical properties, and whether they can change the natural functions of cell membranes. The largely flexible character of lipid aggregation systems results from the low energetic barrier of rearrangement of the lipid structures, strongly dependent on chemical composition.^{10–16} It was shown that both PPDP and 3-pentadecylphenol, as amphiphilic compounds, can easily build into the lipid bilayer.^{17–19} In our previous studies, we stated that the 3-pentadecylphenol changes significantly the lipid phase transitions, induces phase separation, and forms a new type of aggregates like micelles.^{17–19} The IR spectroscopic studies of the DPPC membranes mixed with PPDP demonstrated the influence of the piperidine Mannich base mainly on the *trans/gauche* conformation of lipid hydrocarbon chains.¹⁷ In this paper, we reveal further effects of PPDP on the properties of the DPPC liposomes. In order to understand better the thermo-structural behavior of water dispersion of the DPPC liposomes mixed with different mol % of PPDP, differential scanning calorimetry (DSC) was carried out. To confirm the existence of the phase separation in the new PPDP/DPPC membranes, fluorescence spectroscopy measurements were performed, using Laurdan as a probe. A new type of phases was proposed to be formed in the presence of the piperidine Mannich base molecules.

Received: December 1, 2012

Revised: February 15, 2013

Published: February 20, 2013



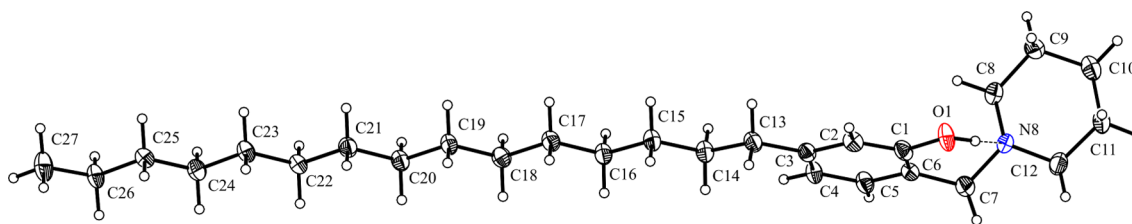


Figure 1. The structure and atom-numbering scheme for the PPDP molecule. The intramolecular O1—H1...N8 contact, stabilizing the PPDP structure, is shown as a dashed line.

2. MATERIALS AND METHODS

The dipalmitoylphosphatidylcholine (DPPC) was purchased from Avanti Polar Lipids, Germany, with a purity of >99.8%. The fluorescence probe Laurdan (2-(dimethylamino)-6-dodecanoyl-naphthalene) was purchased from Molecular Probes (Eugenie, OR) and the 3-pentadecylphenol (PDP) was obtained from Sigma-Aldrich, Germany, both with a purity of >95%. All compounds were used without further purification procedure. The 5-pentadecyl-2-((piperidin-1-yl)methyl)phenol (PPDP) was a product of Mannich condensation of 3-pentadecylphenol, formaldehyde, and secondary amine. The synthesis was performed according to refs 20 and 21. After crystallization from methanol/water (1:1) solution, the next step for checking and/or further purification of the product was the TLC procedure on silica gel G type 60 with a solvent composition of EtOAc/light petroleum/NH₄OH (50:50:7). The rest of the chemicals used in the experiments were of analytical grade.

2.1. X-ray Structure Analysis. The X-ray data were collected at 100 K using an Xcalibur PX diffractometer (ω and φ scan technique).²² The experimental details and the crystal data are given in Table S1 (Supporting Information). The structure was solved by direct methods and refined by full-matrix least-squares on F^2 using the SHELXTL package.²³ All non-hydrogen atoms were refined with anisotropic thermal parameters. All hydrogen atoms were positioned geometrically and added to the structure factor calculations but were not refined. Crystallographic data for the structural analyses reported in this paper have also been deposited with the Cambridge Crystallographic Data Centre (CCDC), number 903461. Copies of the information may be obtained free of charge from the Director, CCDC, 12 Union Road, Cambridge CB2 1EZ, U.K. (fax: +44-1223-336033; e-mail: deposit@ccdc.cam.ac.uk; home page: <http://www.ccdc.cam.ac.uk>).

2.2. Preparation of Liposomes. Small unilamellar vesicles (SUVs) with a varying PPDP/lipid composition have been prepared. Mixed compounds from stock solutions in chloroform were dried under a stream of nitrogen. The residual solvent was removed under a vacuum for 2 h. Dry lipid films were hydrated by the addition of 1 mL of 10 mM phosphate buffer, pH 7.2, during 10 of the cooling/heating processes. Finally, liposomal suspensions were extruded through the filter with 100 nm in the diameter of pores (LiposoFast with polycarbonate filter, Avestin, Canada).

2.3. Fluorescence Measurements. The DPPC liposomes mixed with 30 mol % PPDP compound were prepared as described above. Unilamellar liposomes with a diameter of about 100 nm were incubated with Laurdan fluorescence probe in darkness for 30 min at room temperature. The final concentration of Laurdan was 1.5 and 200 μ M for phospholipid. The steady state emission and excitation spectra

of Laurdan were performed with a Perkin-Elmer LS 50-B spectrofluorimeter, equipped with a thermostatted cell holder. For temperature-dependent fluorescence intensity measurements, the excitation wavelength was 390 nm. The emission spectra were acquired over the range 400–560 nm. The excitation wavelength was 320–400 nm for the fluorescence excitation wavelength dependence studies. The Laurdan generalized polarization (GP) was calculated using the following equation adapted from the work of Parasassi et al.^{24,25}

$$GP = (I_{440} - I_{490}) / (I_{440} + I_{490})$$

where I_{440} and I_{490} are the fluorescence emission intensities at the blue and red edges of the emission spectrum, respectively.

Temperature-dependent intensity of the steady-state fluorescence emission and anisotropy of PPDP molecules in water dispersion of the DPPC liposomes was obtained using a PiStar-180 spectrometer (applied Photophysics, U.K.) equipped with a Peltier temperature controller. The excitation wavelength was generally set to 280 nm.

2.4. DSC Measurements. The SUV liposomes with different PPDP contents were prepared as described above. The final PC lipid concentration was 5 mg/mL. The calorimetric scans were recorded using the VP-DSC microcalorimeter. Individual samples were scanned six times for up scans and six times for down scans. A scan rate was 90 and 60 $^{\circ}$ C/h for heating and cooling cycles, respectively. The prescan and postscan thermostat was set at 15 and 10 min, respectively. The samples were measured immediately after preparation. The obtained endotherms were analyzed by using the Grams software. The area under the transition profiles was used to calculate the molar enthalpy change accompanying phase transition (called further the transition enthalpy).

3. RESULTS

3.1. The Crystal Structure of PPDP Compound. The asymmetric unit of PPDP contains one molecule, as shown in Figure 1. The piperidine ring adopts a chair conformation, as confirmed by the Cremer and Pople puckering parameters,²⁶ or the endocyclic torsion angles shown in Table 1. The angle with the Cremer and Pople plane normal of the N8–C8 bond of 72.92(2) $^{\circ}$ affirmed an equatorial orientation of the 2-methyl-5-pentadecylphenol groups attached to the heterocyclic ring. The dihedral angle between the least-squares plane of the aromatic ring and the pentadecyl part equals 5.7(2) $^{\circ}$. The largest deviations from planarity are observed for peripheral C13 and C27 atoms of hydrophobic chain with values of 0.203(3) and 0.169(3) \AA , respectively. In the PPDP molecule, there is a strong intramolecular hydrogen bond of O–H...N type, characteristic of the Mannich bases.^{27–29}

The arrangement of the PPDP molecules in the crystal unit is mainly determined by the weak C–H...C interactions. Such

Table 1. Selected Geometric Parameters for PPDP Molecule in Crystalline State

Cremer and Pople puckering parameters (\AA , deg)	endocyclic torsion angle (deg)		
Q	0.569(3)	N8—C8—C9—C10	-56.0(3)
q_2	0.020(3)	C8—C9—C10—C11	53.5(3)
q_3	-0.568(3)	C9—C10—C11—C12	-53.0(3)
θ	177.9(3)	C10—C11—C12—N8	56.6(3)
φ_2	160(7)	C11—C12—N8—C8	-59.5(3)
		C12—N8—C8—C9	58.2(3)

contacts, shorter than the sum of the van der Waals radii for the H and C, are summarized in Table 2. As presented in Figure 2,

Table 2. Hydrogen Bond and Weak Contact Geometry (\AA , deg) in Crystal^a

D—H...A	D—H	H...A	D...A	D—H...A
O1—H1...N8	0.84	1.97	2.690(3)	144
C7—H7A...C2 ⁱ	0.99	2.74	3.601(4)	146
C13—H13A...C5 ⁱⁱ	0.99	2.86	3.716(4)	146
C11—H11A...C5 ⁱⁱⁱ	0.99	2.84	3.812(4)	169

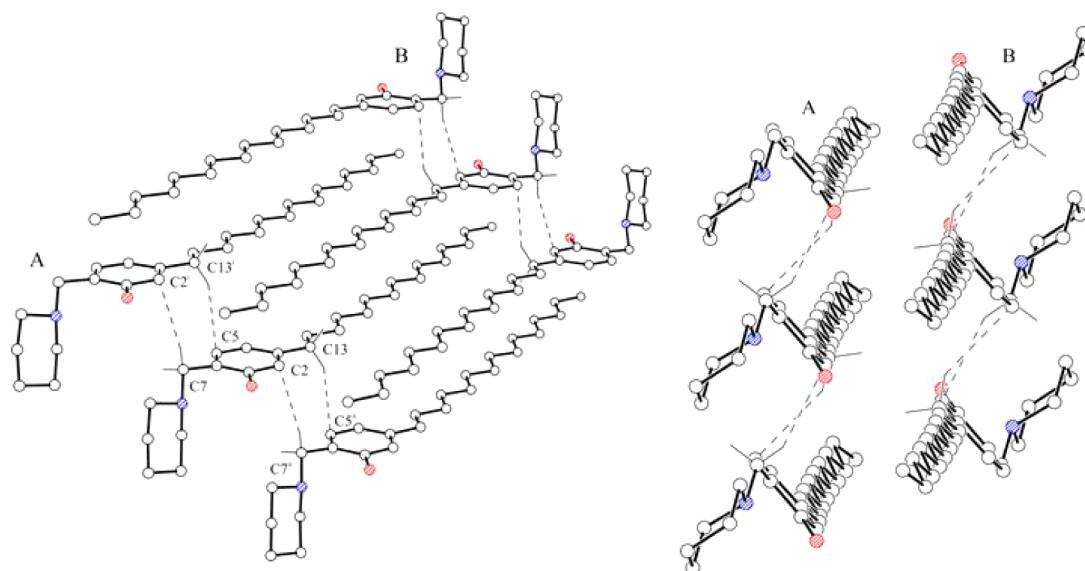
^aSymmetry codes: (i) $x - 1, y, z$; (ii) $x + 1, y, z$; (iii) $-x + 1, -y, -z$.

the weak contacts located in the area of the polar head of PPDP link the adjacent molecules into infinite chains, realized by the action a -axis translation, which leads to the formation of intermolecular interdigitation of pentadecyl side chains. It is noteworthy that intra- and interplanar distances between the planes defined by neighboring pentadecyl chains are, respectively, 3.66 and 3.94 \AA . A similar arrangement of the side chains has been previously observed for 6-*n*-pentadecyl-2,4-dihydroxy-benzoic acid³⁰ and 4-cyano-4'-*n*-dodecylbiphenyl,³¹ which accounts for the tendency to favor the formation of the intermolecular interdigitation pattern in the solid state.

The large contributions to the formation of the interdigitated layers are also weak contacts between the methyl-piperidine groups and C atoms of aromatic rings; see Figure 3A. A clearly

visible graphical representation of that head-to-head interaction between neighboring PPDP molecules is shown in Figure 3B.

3.2. The Effect of the PPDP on the Phase Behavior of DPPC Liposomes. The calorimetric behavior of the PPDP/DPPC mixtures with an increasing mole concentration of the Mannich base component is shown in Figure 4. For the pure DPPC liposomes, the pretransition (T_p) and main phase transition (T_m) were monitored at 34.5 and 41.5 $^{\circ}\text{C}$, respectively. Only in the lowest mole fraction of PPDP (up to 10 mol %), the broad with a low intensity pretransition peak was still observed. Additionally, in liposomes doped with 10 mol % of the compound under study, a small and flat deviation from the baseline was also observed near the temperature 29 $^{\circ}\text{C}$. The rise of the PPDP content in the DPPC membranes was accompanied by the splitting of the main phase transition peak into two main subprofiles fitted with the Lorentz function. Phase separation into two main subcomponents begins to be clearly visible in the mixture of 20 mol % PPDP (Figure 4). With the increase of the PPDP/DPPC mole ratio, the contribution of the lower temperature process becomes gradually more prominent, which may be seen in the evolution of the shape of the DSC thermograms in Figure 4. As the concentration of the admixture was increased, the position of the maximum of the low temperature peak was slightly shifted to the higher temperature, from around 35 $^{\circ}\text{C}$ (20 mol % PPDP) to 36 $^{\circ}\text{C}$ in the PPDP-rich membranes (Figure 5A). The similar half-width of that peak around 1.6 $^{\circ}\text{C}$ was almost 2 times narrower than that for the corresponding high-temperature profile. The second subcomponent was represented by a high-temperature subpeak, and it had a similar maximum position, centered at around 38.5 $^{\circ}\text{C}$ for all mixed systems with the exception of liposomes with 10 mol % PPDP, where T_m was approximately 1 $^{\circ}\text{C}$ higher (see Figure 5A). Additionally, the half-height width of the high temperature DSC profile rose with the increase of the mole fraction of the admixture, from around 2 $^{\circ}\text{C}$ for 10/90 mol % mole ratio of the Mannich base to the DPPC molecules to more than 3.5 $^{\circ}\text{C}$ for 30/70 and 50/50 mol % mixtures. The proportion of the value of transition enthalpy (ΔH) for the PPDP/DPPC liposomes under scrutiny and of the value of the DPPC transition enthalpy (ΔH_0) changed as a

**Figure 2.** Structural interdigitated motif created by the interpenetrated A and B layers arranged by weak C—H...C interactions.

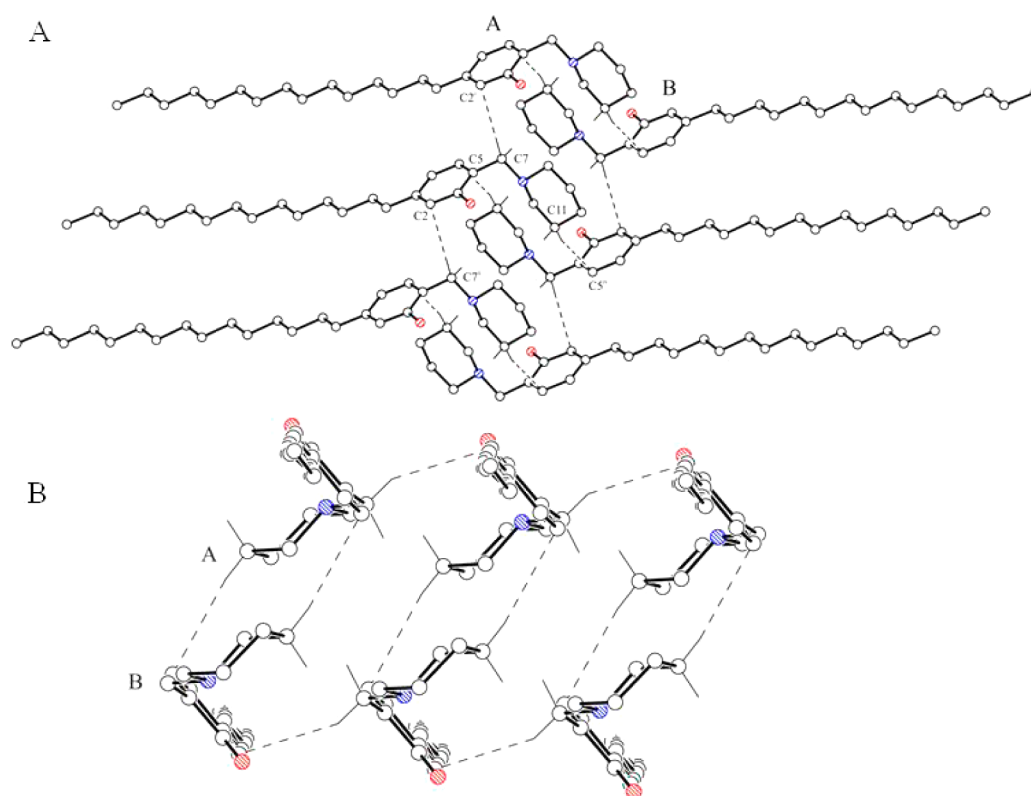


Figure 3. Packing motif created by head-to-head interaction between neighboring PPDP molecules effectuated by weak contacts leading to the formation of an infinite chain.

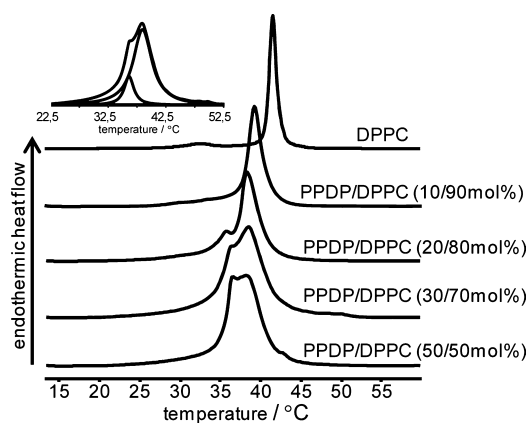


Figure 4. The DSC thermograms of DPPC lipids in the presence of different mol % of PPDP. Inset: an example of thermogram (PPDP/DPPC, 30/70 mol %) deconvolution.

function of doped compound concentration. That is illustrated in Figure 5B, in which the relative enthalpy ($\Delta H/\Delta H_0$) is plotted versus the mole concentration of PPDP. The relative enthalpy for the high temperature component manifested a biphasic behavior in the function of the PPDP content. This value first decreases in a low range of mol % of the compound under study, and then increases for the mixtures with more than 20 mol % of the long chain phenol Mannich base. The second, low-temperature component, as opposed to the first one, was accompanied by a sharp and high growth of its transition enthalpy, which proves that with the increase of PPDP mol % the $\Delta H/\Delta H_0$ rapidly increases.

3.3. Laurdan Fluorescence Studies. Laurdan (2-dimethylamino-6-lauroyl-naphthalene) is a fluorescence probe

sensitive to the polarity and mobility of its environment. The characteristic fluorescence properties of Laurdan result from the availability of the solvent molecules surrounding the fluorescent naphthalene residue to form the dipole states and to reorientate along the probe's excited state dipole.^{25,25,32} As the concentration and molecular dynamics of water molecules located in lipid bilayers differ in gel and liquid-crystal states of membranes, the Laurdan is widely used for monitoring phase transitions, domain formation, and changes in the hydration, polarity, fluidity, and order of lipid membranes.^{24,25,32} The 12-carbon aliphatic tail anchors the naphthalene moiety at the level of the phospholipid glycerol backbone. Few water molecules present in this region of the lipid bilayer are responsible for dipolar relaxation of probe molecules. In the gel phase, the locally excited state gives the emission with the maximum value in the blue region. In the liquid-crystalline condition, the increase of hydration and mobility of the lipid membrane results in the red-shifted emission that originated from the formation of a charge transfer excited state, stabilized by the water dipole reorientation process. Additionally, in the lipid environment, in the ground state, there are Laurdan molecules with and without partial charge separation, stabilized by surrounding dipoles. Thus, the plot of the GP values versus the excitation wavelength provides the quantitative information on the proportion of the Laurdan molecules surrounded by the gel or the fluid phase of phospholipids. The emission spectra of Laurdan in the low- and high-temperature phase states of the pure DPPC and PPDP/DPPC liposomes are shown in Figure 6A and B, respectively. The blue emission band in both types of liposomes has a maximum value of approximately 440 nm and shifts to the red part with the increase of temperature. In the liquid crystalline phase of the pure DPPC bilayer, one band

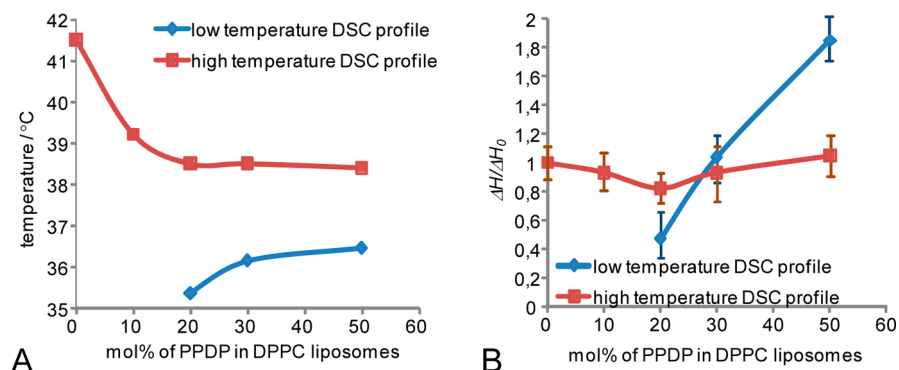


Figure 5. The evolution of the phase transition temperatures (A) and the relative enthalpy changes ($\Delta H/\Delta H_0$) (B) for two subcomponents present in DPPC liposomes mixed with different PPDP mol %. Errors are given as standard deviation values of six measurements.

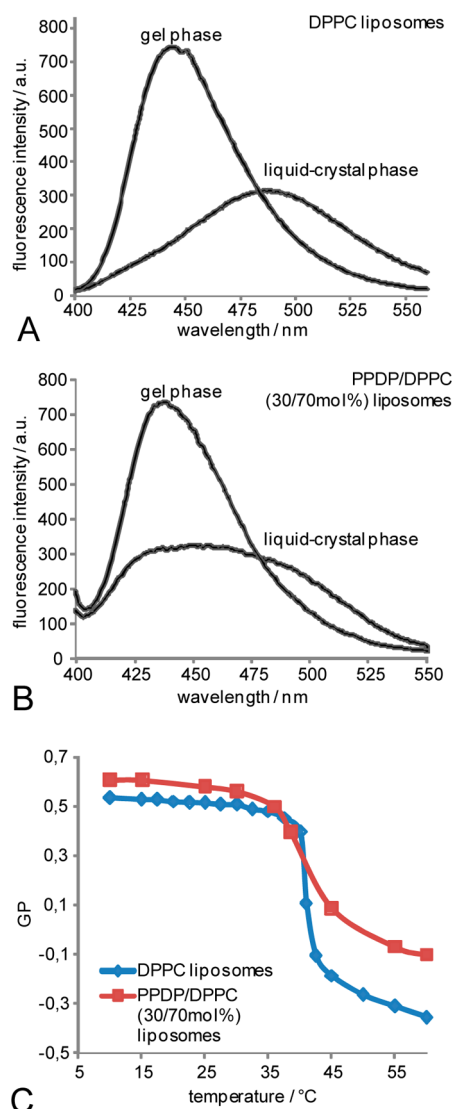


Figure 6. The Laurdan emission band in the pure DPPC (A) and PPDP/DPPC (30/70 mol %) (B) liposomes. The Laurdan generalized polarization (GP) values as a function of the temperature for the pure and PPDP-mixed DPPC vesicles. The excitation wavelength was 390 nm.

with the maximum at 490 nm is observed. However, in the mixture of 30 mol % PPDP with 70 mol % DPPC, there is still the blue emission band which coexists with the red emission

one, characteristic for a fluid lipid phase. Figure 6C presents the GP values for $\lambda_{\text{ex}} = 390$ nm plotted as a function of temperature for the pure and mixed DPPC liposomes. The sharp decrease of GP marks the temperature of the main phase transition in the DPPC bilayers, whose value is around 41.5 °C, the same as obtained from the DSC measurement. The presence of the compound under study in the lipid membrane induces more gradual reduction of the GP values in the range of phase transition temperature. Below the phase transition of the pure DPPC membrane, the values of GP lie around 0.55, at the temperature of main phase transition reaching almost zero, and finally, in the fluid state, they adopt a position of about -0.3 .^{24,25,32} In the PPDP/DPPC mixture, in a lower temperature range, GP slightly shifts to higher values as compared with the pure DPPC membranes, and at the highest temperatures, it assumes a value of -0.1 , which significantly differs from the GP of pure DPPC liposomes. The GP profiles of emission of Laurdan in the function of the wavelength of excitation for the pure and PPDP-mixed DPPC liposomes at different temperatures are presented in Figure 7. In the gel phase of the DPPC membrane, the GP values constitute a straight line, whereas, for liquid crystalline state, GP becomes a descending function of λ_{ex} . The slope of GP versus λ_{ex} relationship is positive when different phases coexist inside the system. Differently from the pure DPPC, the ascending dependence of the GP versus λ_{ex} was present already at the temperatures before the phase transition, which indicates the non-homogeneity of the PPDP-doped DPPC membranes in the gel phase.

3.4. Photophysics of PPDP in DPPC Liposomes. The PPDP compound has the aminomethyl-phenol moiety, which is the source of its intrinsic fluorescence. Within one molecule, there is a proton-donor OH group in the neighborhood of the proton-acceptor center - nitrogen atom of the piperidine moiety, which makes it possible to form an intermolecular hydrogen bond in the "head" part of the PPDP molecule. The strong O—H...N interaction was already proved by the presence of a broad ν_{OH} band, centered at around 2800 cm^{-1} in the PPDP dry film exposed on the ZnSe crystal in the IR-ATR experiments.¹⁷ Additionally, in the crystalline state of PPDP, the relatively short distance between O and N atoms, equal to 2.689(3) Å, indicates the strong H-bond interaction. Previous fluorescence studies performed on different derivatives of the Mannich bases have indicated that the excited state intramolecular proton transfer process is influenced by solvent molecules and it is more pronounced in the polar solvents (ref 29 and articles cited therein). The dual fluorescence was observed from the PPDP molecules incorporated into the fully

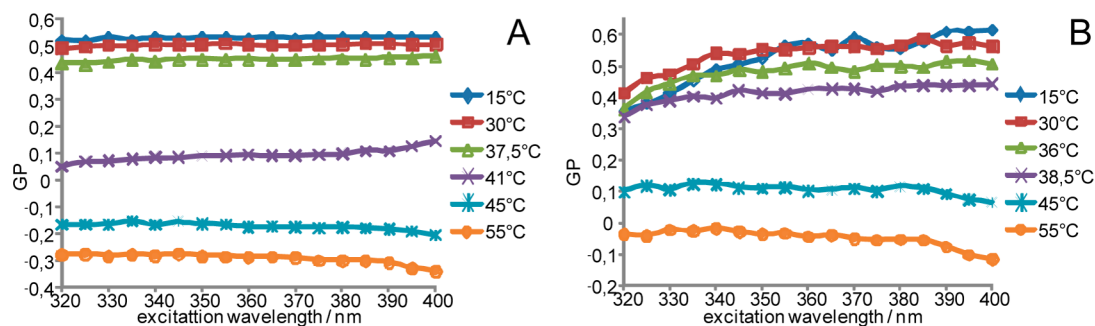


Figure 7. Generalized polarization values for Laurdan in the pure DPPC liposomes (A) and with addition of 30 mol % PPDP as a function of excitation wavelength at different temperatures.

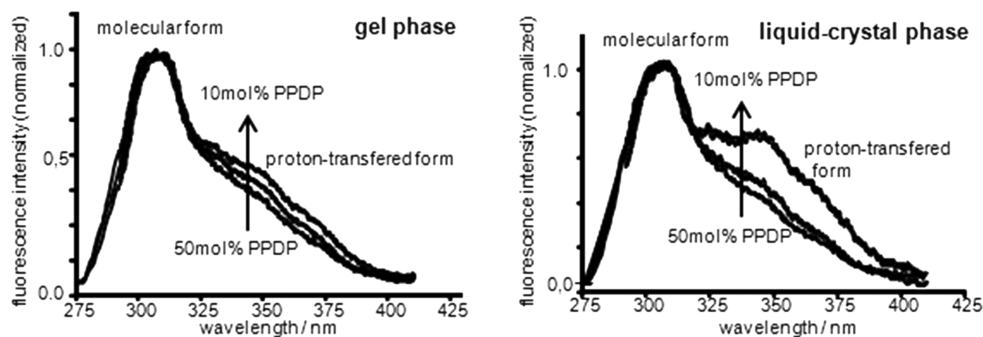


Figure 8. Fluorescence emission spectra of PPDP molecules in DPPC liposomes in gel (A) and liquid crystal phase (B). The DPPC vesicles had the 10, 30, and 50 mol % Mannich base. The excitation wavelength was 280 nm.

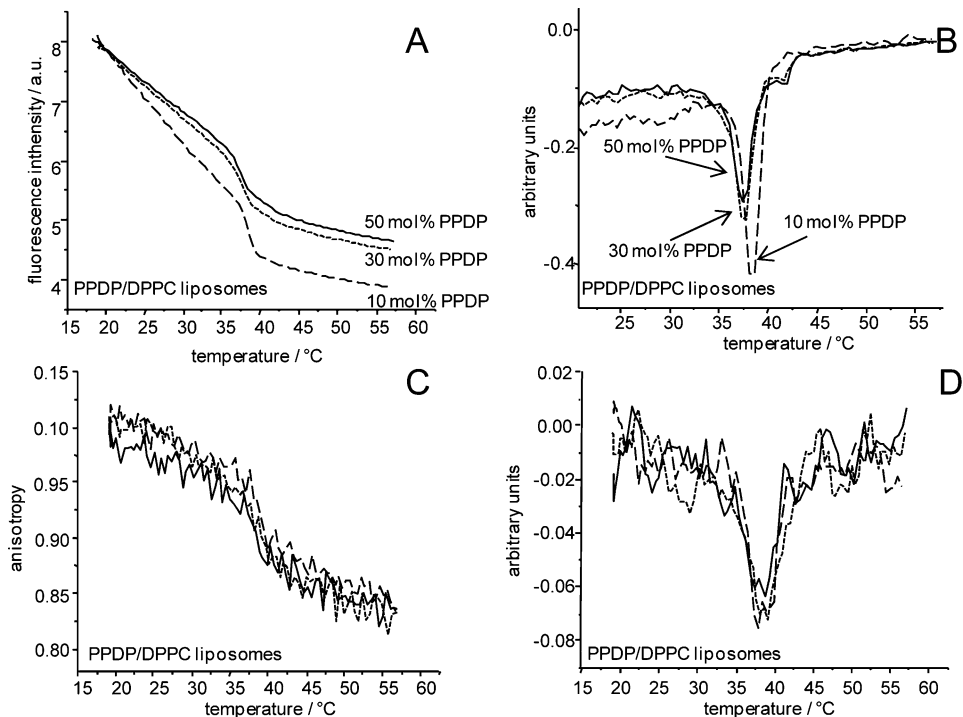


Figure 9. (A) Temperature dependence of the fluorescence intensity for different concentrations of PPDP in DPPC: 10 (dashed line), 30 (dotted line), and 50 mol % (solid line). An integrated (total) fluorescence intensity of PPDP at excitation wavelength $\lambda_{\text{ext}} = 280$ nm was measured. (B) The first derivative of the fluorescence intensity curves is shown in part A. (C) Temperature dependence of the fluorescence anisotropy for different concentrations of PPDP in DPPC: 10 (dashed line), 30 (dotted line), and 50 mol % (solid line). (D) The first derivative of the fluorescence anisotropy curves is shown in part C.

hydrated DPPC bilayers (see Figure 8). In general, the fluorescence properties of PPDP in liposomes were similar to other aminomethyl-phenols dissolved in polar solvents (like

water and alcohols), when the excited state proton-transfer reaction was present.²⁹ In both the gel and liquid-crystal phases of the DPPC bilayer, two fluorescence bands of PPDP coexist.

The blue emission band centered at around 328 nm originates from the neutral (molecular) form of long chain phenol Mannich base. The second emission band, with the maximum value at around 370 nm, is ascribed to the ionic, proton-transferred form present in the excited state. Figure 9A and B display, respectively, the temperature dependence of the PPDP fluorescence intensity and of its first derivative for various PPDP concentrations in DPPC liposomes. The quenching of the intensity of the PPDP fluorescence was observed as a function of increasing temperature. Additionally, a sharp decrease of emission intensity was noticed at the approximate temperature of transition of PPDP/DPPC liposomes. The maximum of the peak of the first derivative allowed us to determine the temperature of phase transition for all the PPDP/DPPC water mixtures under study. The intensity of the derivative profile decreased with the rise of the mol % contribution of the Mannich base in liposomes. During the heating process, the conformational fluidization is accompanied by the increase of the hydration of lipid bilayer, especially at the temperature of chain-melting lipid phase transition, when this process has a dramatic course. Thus, the polarity of the environment of PPDP in the DPPC membranes has an influence on the photophysics of the compound under study. For a lower mol % of PPDP, the proportion of the intensity of the blue emission band to the red one was higher in the gel state, in comparison to a more disordered and highly hydrated liquid-crystalline phase (see Figure 8). When the concentration of the Mannich base reached 30 or 50 mol %, this difference faded away. Figure 9C,D presents the temperature dependence of the phenol Mannich base fluorescence anisotropy data and their first derivatives 10, 30, and 50 mol % PPDP in the DPPC liposomes. The thermal evolution of the values of the fluorescence anisotropy was independent of the PPDP concentration in the lipid membrane. The gradual decrease of anisotropy present in the outside of the region of phase transition was broken at the temperature of phase transition. The abrupt increase of the mobility of the phenol-2 piperidine moiety marks the main phase transition of doped liposomes.

4. DISCUSSION

The phase separation shown by the splitting of the DSC profile of the PPDP/DPPC liposomes into two main subpeaks can possibly mean that either the whole system undergoes two separate transitions, one after another, or that there are two separate regions (domains) with different chemical compositions and/or different structures, and each of them is subject to its own phase transition. The Laurdan fluorescence measurements clearly showed the non-homogeneous gel phase in the PPDP-mixed DPPC systems. The positive $GP(\lambda_{ex})$ slope at the temperatures below T_m indicates a mixture of different quasi-gel phases present in separate domains. The simplest event that could result in the domain formation would be the presence of the PPDP-rich and PPDP-poor regions inside the membrane, attributed to the incomplete miscibility of these two components, analogous to cholesterol-phospholipid and to many other systems.^{12,13,33–35} The PPDP-poor regions show the biphasic evolution of the relative enthalpy ($\Delta H/\Delta H_0$) as a function of the PPDP content (see Figure 5). At a lower Mannich base concentration, the relative enthalpy of the high-temperature DSC peak decreases with the increase of the concentration of doped compound. However, from 20 mol % PPDP, the characteristic growth of the enthalpy indicates the formation of a new phase in the PPDP/DPPC bilayers. As one

of the basic features of the occurrence of the interdigitation phase in many different lipid-containing systems is the growth of the transition enthalpy,^{36–38} the interdigitation can be one of the possible processes to be considered in the system under study. The growth of the relative enthalpy is more evident in the second type, i.e., the PPDP-rich domains. It starts to be present in 20 mol % PPDP–DPPC mixtures, when the second, low-temperature thermogram arises. A sharper growth of the relative enthalpy of the low-temperature component indicates a higher contribution of the more promoted, PPDP-rich, newly formed domains.

In a higher temperature range, over T_m , in the PPDP/DPPC liposomes, the GP values are a descending function of excitation wavelength, which is typical for the liquid crystalline phase of the pure DPPC. However, the GP values are distinctly higher than those for the pure DPPC liposomes in the fluid state, which accounts for the lower hydration state and/or lower fluidization of the liquid crystalline phase of the PPDP-mixed lipid membranes. The comparison of the steady-state fluorescence of the PPDP molecules in gel and liquid-crystal phases for different mol % of the PPDP content in the DPPC bilayer showed the decrease of the polarity of the systems under study, with the rise of the concentration of the long chain Mannich base which are less polar molecules than DPPC. The contribution of the proton transfer reaction in the excited state, which strongly depends on the polarity of the environment,²⁹ decreases with the growth of PPDP mol % in lipid bilayers. That feature is manifested by the lowering of the intensity of the red emission band in Figure 8. After the chain-melting phase transition, the polarity of the PPDP environment increased evidently in the liquid-crystal state as compared with the gel phase, only for mixtures with a lower PPDP content. On the other hand, the main phase transition of the DPPC bilayer, as is commonly known, is accompanied by the increase of the fluidization and hydration of the membrane, which causes the lower increase of population of the excited state proton transfer form than in the DPPC membranes mixed with 30 and 50 mol % PPDP. The similar evolution of the fluorescence anisotropy of PPDP in the whole temperature range for 10, 30, and 50 mol % PPDP suggests that the admixture can change only the polarity of the lipid membrane without noticeable alterations of the order parameter (see Figure 9C,D). The measured values of the PPDP anisotropy averaged the output signal over the whole liposomes, where the phase separation is present. Therefore, it is difficult to state clearly whether the emerging phases are not accompanied by distinct changes of arrangement of the PPDP–DPPC aggregates. It is commonly known from different studies of structures of micelles or hexagonal phases that their formation should be manifested by a considerable difference in anisotropy values, as compared with the one for the pure DPPC bilayers. On the other hand, the interdigitated state can be accompanied by minor anisotropy changes.

The crystallographic data showed the favorable three-dimensional packing of the PPDP molecules. The geometry of this compound allows tight packing in both polar and apolar regions of PPDP aggregates. The PPDP molecules in the crystal cell have the hydrocarbon chains in the long expanded *trans* state. The close contacts of hydrophobic tails were allowed due to the interdigitated process, which is clearly a consequence of the larger energy gain from the strongest van der Waals interactions. In the interdigitated state, the molecules from one monolayer interpenetrate the free spaces between molecules of

the opposing layer. That phenomenon can be observed in different long-chain amphiphilic molecules, for example, phospholipids. The DPPC bilayers can adopt the gel interdigitated phase ($L_{\beta}I$) in the presence of surface active molecules or in higher pressure conditions.^{36,39–41} The methanol, ethanol, or acetonitrile molecules create a small void which can be entered by the hydrocarbon chains from phospholipids in the opposing layer.^{36,39–41} The incorporation of the PPDP molecules into the DPPC bilayer leads to the distinct changes of the structure and physicochemical properties of lipid membranes, as shown in the above-presented microcalorimetric and fluorescence studies. The PPDP molecules have a conical shape. The relatively large volume of the hydrophilic head, as compared with the narrow but long tail, can induce the formation of energetically undesirable “free volume” between the tails in the hydrophobic region of mixed bilayers. Filling these gaps with the chains from the hydrophobic region leads to the formation of new phases in studied mixtures. Different types of structures of the PPDP/DPPC aggregates can be expected. If free volumes are reduced when the free spaces between tails of one monolayer are interpenetrated by the chains from the opposing one, then the interdigitated phase can be formed. Additionally, at higher mol % of the Mannich base, as a result of the nonuniform distribution of the admixture, there are regions consisting mainly of PPDP molecules, which can aggregate in a similar manner as in the crystal state.

The obtained results can be summarized as follows:

- (1) The phase separation shown by the splitting of the main phase transition peak and the increase of the transition enthalpy, together with the positive $GP(\lambda_{ex})$ slope in the gel phase, indicate that PPDP introduces the PPDP-rich and -poor domains in lipid membranes with different physicochemical properties. Direct determination of the type of new phases still requires additional research like X-ray or proton scattering studies. However, the presence of an interdigitation phase can be supported by the characteristic rise of relative enthalpy and by the fact that other hydrocarbon chains slide between one another in the favored form of the aggregation of the PPDP molecules in the crystal state, which can also be adapted in the lipid bilayer system.
- (2) The long chain Mannich base has an influence of the DPPC bilayer structure in the gel and liquid crystal form. Both phases are less polar in the presence of the compound under study.

■ ASSOCIATED CONTENT

📄 Supporting Information

Table S1 with the decryption of crystal and data collection parameters. This material is available free of charge via the Internet at <http://pubs.acs.org>.

■ AUTHOR INFORMATION

Corresponding Author

*Phone: +48 71 375 7209. Fax: +48 71 328 2348. E-mail: kasia_cieslik0@yahoo.com.

Notes

The authors declare no competing financial interest.

■ ACKNOWLEDGMENTS

This work was supported by the Foundation for Polish Science - the programme POMOST, cofinanced by the European Union within European Regional Development Fund (V edition 2012) and by Grant No. N N204 150338 from the National Science Centre. We thank the ÖAD (Proj. PL-05/2011) and Polish Ministry of Science and Higher Education (grant-in-aid for scientific research and development for young scientists, 2012) for additional financial support.

■ ABBREVIATIONS USED

DPPC - 1,2-dipalmitoyl-*sn*-glycero-3-phosphocholine; PPDP - 5-pentadecyl-2-((piperidin-1-yl)methyl)phenol; DSC - differential scanning calorimetry; SUV - small unilamellar vesicles

■ REFERENCES

- (1) Joshi, S.; Khosla, N.; Tiwari, P. In Vitro Study of Some Medically Important Mannich Bases Derived from Antitubercular Agent. *Bioorg. Med. Chem.* **2004**, *12*, 571–576.
- (2) Lopes, F.; Capela, R.; Goncaves, J. O.; Horton, P. N.; Hursthouse, M. B.; Iley, J.; Casimiro, C. M.; Bom, J.; Moreira, R. Amidomethylation of Amodiaquine: Antimalarial N-Mannich Base Derivatives. *Tetrahedron Lett.* **2004**, *45*, 7663–7666.
- (3) Ferlin, M. G.; Chiarello, G.; Antonucci, F.; Caparrotta, L.; Frolidi, G. Mannich Bases of 3H-Pyrrolo[3,2-f]quinoline Having Vasorelaxing Activity. *Eur. J. Med. Chem.* **2002**, *37*, 427–434.
- (4) Malinka, W.; Swiatek, P.; Filipek, B.; Sapa, J.; Jezierska, A.; Koll, A. Synthesis, Analgesic Activity and Computational Study of New Isothiazolopyridines of Mannich Base Type. *Farmaco* **2005**, *60*, 961–968.
- (5) Holla, B. S.; Veerandra, B.; Shivanada, M. K.; Poojary, B. Synthesis Characterization and Anticancer Activity Studies on Some Mannich Bases Derived from 1,2,4-Triazoles. *Eur. J. Med. Chem.* **2003**, *38*, 759–67.
- (6) Filler, R.; Kobayashi, Y. *Biomedical Aspects of Fluorine Chemistry*; Elsevier: Amsterdam, The Netherlands, 1982.
- (7) Castillo, J. A.; Pinazo, A.; Carilla, J.; Infante, M. R.; Alsina, M. A.; Haro, I.; Clapes, P. Interaction of Antimicrobial Arginine-Based Cationic Surfactants with Liposomes and Lipid Monolayers. *Langmuir* **2004**, *20*, 3379–3387.
- (8) Negm, N. A.; Morsy, S. M. I.; Said, M. M. Biocidal Activity of Some Mannich Base Cationic Derivatives. *Bioorg. Med. Chem.* **2005**, *13*, 5921–5926.
- (9) Finar, I. L. *Organic Chemistry, Part 1: Fundamental Principles*; ELBS: New York, 1995.
- (10) Szwed, J.; Cieřlik-Boczula, K.; Czarnik-Matusiewicz, B.; Jaszczyszyn, A.; Gęsiorowski, K.; Świątek, P.; Malinka, W. Moving-Window 2D Correlation Spectroscopy in Studies of Fluphenazine-DPPC Dehydrated Film as a Function of Temperature. *J. Mol. Struct.* **2010**, *974*, 192–202.
- (11) Murawska, A.; Cieřlik-Boczula, K.; Czarnik-Matusiewicz, B. Interactions in Two-Component Liposomes Studied by 2D Correlation Spectroscopy. *J. Mol. Struct.* **2010**, *974*, 183–1915.
- (12) Cieřlik-Boczula, K.; Szwed, J.; Jaszczyszyn, A.; Gęsiorowski, K.; Koll, A. Interactions of Dihydrochloride Fluphenazine with DPPC Liposomes: ATR-IR and ³¹P NMR Studies. *J. Phys. Chem. B* **2009**, *113*, 15495–15502.
- (13) Cieřlik-Boczula, K.; Maniewska, J.; Gryniewicz, G.; Szeja, W.; Koll, A.; Hendrich, A. Interaction of Quercetin, Genistein and Its Derivatives with Lipid Bilayers - An ATR IR-Spectroscopic Study. *Vib. Spectrosc.* **2012**, *62*, 64–69.
- (14) Yue, X.; Chen, X.; Li, Q. Comparison of Aggregation Behaviors of a Phytosterol Ethoxylate Surfactant in Protic and Aprotic Ionic Liquids. *J. Phys. Chem. B* **2012**, *116*, 9439–9444.
- (15) Oldham, E. D.; Xie, W.; Farnoud, A. M.; Fiegel, J.; Lehmler, H.-J. Disruption of Phosphatidylcholine Monolayers and Bilayers by Perfluorobutane Sulfonate. *J. Phys. Chem. B* **2012**, *116*, 9999–10007.

- (16) Yamamoto, E.; Akimoto, T.; Shimizu, H.; Hirano, Y.; Yasui, M.; Yasuoka, K. Diffusive Nature of Xenon Anesthetic Changes Properties of a Lipid Bilayer: Molecular Dynamics Simulations. *J. Phys. Chem. B* **2012**, *116*, 8989–8995.
- (17) Ciesik, K.; Koll, A.; Grdadolnik, J. Structural Characterization of a Phenolic Lipid and Its Derivative Using Vibrational Spectroscopy. *Vib. Spectrosc.* **2006**, *41*, 14–20.
- (18) Cieřlik-Boczula, K.; Küpçü, S.; Rünzler, D.; Koll, A.; Köhler, G. Effects of The Thenolic Lipid 3-Pentadecylphenol on Phospholipid Bilayer Organization. *J. Mol. Struct.* **2009**, *919*, 373–380.
- (19) Cieřlik-Boczula, K.; Koll, A. The Effect of 3-Pentadecylphenol on DPPC Bilayers ATR-IR and ^{31}P NMR Studies. *Biophys. Chem.* **2009**, *140*, 51–56.
- (20) Tychopoulos, V.; Tyman, J. H. P. Enhancement of the Rate of Mannich Reactions in Aqueous Media. *Synth. Commun.* **1986**, *16*, 1401–1409.
- (21) Short, E. L.; Tychopoulos, V.; Tyman, H. P. Long Chain Phenols—Part 30: A Rate Study of the Mannich Reaction of Phenols (With Particular Reference to 3-Pentadecylphenol). *J. Chem. Technol. Biotechnol.* **1992**, *53*, 389–396.
- (22) Oxford Diffraction Ltd. (1995–2003). *Xcalibur PX Software – CrysAlis CCD and CrysAlis RED*, version 1.171; Oxford Diffraction Poland: Wrocław, Poland.
- (23) Sheldrick, G. M. A Short History of SHELX. *Acta Crystallogr., Sect. A* **2008**, *64*, 112–122.
- (24) Parasassi, T.; Krasnowska, E. K.; Bagatolli, L.; Gratton, E. Laurdan and Prodan as Polarity-Sensitive Fluorescent Membrane Probes. *J. Fluoresc.* **1998**, *8*, 365–373.
- (25) Parasassi, T.; Stasio, G.; dUbaldo, A.; Gratton, E. Phase Fluctuation in Phospholipid Membranes Revealed by Laurdan Fluorescence. *Biophys. J.* **1990**, *57*, 1179–1186.
- (26) Cremer, D.; Pople, J. A. General Definition of Ring Puckering Coordinates. *J. Am. Chem. Soc.* **1975**, *97*, 1354–1358.
- (27) Martinek, H.; Wolschann, P. Tautomerism of Some Amino-methylphenols in Aqueous Solution. *Bull. Soc. Chim. Belg.* **1981**, *90*, 37–43.
- (28) Koll, A.; Wolshann, P. Steric Modification of the Intramolecular Hydrogen Bond in 2-(Methylimino-phenyl-methyl)-phenols. *Monatsh. Chem.* **1999**, *127*, 475–492.
- (29) Szemik-Hojniak, A.; Koll, A. Intramolecular Excited State Proton Transfer in Mannich Base - 3,5,6-Trimethyl-2(N,N'-diethylaminomethyl) Phenol. *J. Photochem. Photobiol., A* **1993**, *72*, 123–132.
- (30) Gadret, M.; Goursolle, M.; Leger, J. M.; Colleter, J. C. Structure Cristalline du Chlorhydrate de Bupranolol (Chlorhydrate de DL-t-Butylamino-1 (chloro-2' méthyl-5' phénoxy)-3 propanol-2). *Acta Crystallogr., Sect. B: Struct. Crystallogr. Cryst. Chem.* **1975**, *31*, 2784.
- (31) Rajnikant, V. K.; Gupta, R.; Gupta, A.; Kumar, R. K.; Bamezai, N. K.; Sharma, B.; Varghese, B. X-ray Analysis of 4-Cyano-4'-n-dodecylbiphenyl: A Liquid Crystalline Material. *Mol. Cryst. Liq. Cryst. Sci. Technol., Sect. C* **1999**, *11*, 165–170.
- (32) Parasassi, T.; Stasio, G.; Ravagnan, G.; Rusch, R. M.; Gratton, E. Quantitation of Lipid Phases in Mixed Phospholipid Vesicles by Generalized Polarization of Laurdan Fluorescence. *Biophys. J.* **1991**, *60*, 179–189.
- (33) Tampe, R.; Lukas, A.; Galla, H. J. Glycophorin-Induced Cholesterol-Phospholipid Domains in Dimyristoylphosphatidylcholine Bilayer Vesicles. *Biochemistry* **1991**, *30*, 4909–4916.
- (34) Hendrich, A. B.; Wesolowska, O.; Michalak, K. Trifluoperazine Induces Domain Formation in Zwitterionic Phosphatidylcholine but Not in Charged Phosphatidylglycerol Bilayers. *Biochim. Biophys. Acta* **2001**, *1510*, 414–425.
- (35) Lu, N.; Yang, K.; Yuan, B.; Ma, Y. Molecular Response and Cooperative Behavior during the Interactions of Melittin with a Membrane: Dissipative Quartz Crystal Microbalance Experiments and Simulations. *J. Phys. Chem. B* **2012**, *116*, 9432–9438.
- (36) Wu, F.-G.; Wang, N.-N.; Tao, L.-F.; Yu, Z.-W. Acetonitrile Induces Nonsynchronous Interdigitation and Dehydration of Dipalmitoylphosphatidylcholine Bilayers. *J. Phys. Chem. B* **2010**, *114*, 12685–12691.
- (37) Matsingou, Ch.; Demetzos, C. Calorimetric Study on the Induction of Interdigitated Phase in Hydrated DPPC Bilayers by Bioactive Labdanes and Correlation to Their Liposome Stability: The Role of Chemical Structure. *Chem. Phys. Lipids* **2007**, *145*, 45–62.
- (38) Wang, P.; Chen, J.; Hwang, F. Anisodamine Causes Acyl Chain Interdigitation in Phosphatidylglycerol. *FEBS Lett.* **1993**, *332*, 193–196.
- (39) Löbbecke, L.; Cevc, G. Effects of Short-Chain Alcohols on the Phase Behavior and Interdigitation of Phosphatidylcholine Bilayer Membranes. *Biochim. Biophys. Acta* **1995**, *1237*, 59–69.
- (40) Ichimori, H.; Hata, T.; Matsuki, H.; Kaneshina, S. Barotropic Phase Transitions and Pressure-Induced Interdigitation on Bilayer Membranes of Phospholipids with Varying Acyl Chain Lengths. *Biochim. Biophys. Acta* **1998**, *1414*, 165–174.
- (41) Nambi, P.; Rowe, E. S.; McIntosh, T. J. Studies of the Ethanol-Induced Interdigitated Gel Phase in Phosphatidylcholines Using the Fluorophore 1,6-Diphenyl-1,3,5-hexatriene. *Biochemistry* **1988**, *27*, 9175–9182.